TITANOCENE AND *ansa*-TITANOCENE COMPLEXES BEARING 2,6-BIS(ISOPROPYL)PHENOXIDE LIGAND(S). SYNTHESES, CHARACTERIZATION AND USE IN CATALYTIC DEHYDROCOUPLING POLYMERIZATION OF PHENYLSILANE

Michal HORÁČEK[a1], Jan MERNA[b], Róbert GYEPES[c], Jan SÝKORA[d], Jiří KUBIŠTA[a2] and Jiří PINKAS[a3,*]

[a] *J. Heyrovský Institute of Physical Chemistry, Academy of Sciences of the Czech Republic, v.v.i., Dolejškova 2155/3, 182 23 Prague 8, Czech Republic; e-mail: [1] horacek@jh-inst.cas.cz, [2] kubista@jh-inst.cas.cz, [3] pinkas@jh-inst.cas.cz*

[b] *Institute of Chemical Technology, Prague, Department of Polymers, Technická 5, 166 28 Prague 6, Czech Republic; e-mail: jan.merna@vscht.cz*

[c] *Charles University, Department of Inorganic Chemistry, Hlavova 2030, 128 43 Prague 2, Czech Republic; e-mail: gyepes@natur.cuni.cz*

[d] *Institute of Chemical Process Fundamentals, Academy of Sciences of the Czech Republic, v.v.i., Rozvojová 135, 165 02 Prague 6, Czech Republic; e-mail: sykora@icpf.cas.cz*

Received November 3, 2010
Accepted November 23, 2010
Published online January 6, 2011

Aryloxychloro and bis(aryloxy) titanocenes of general formula $L_2TiCl_{2-x}(OAr')_x$ where L = η^5-C_5H_5 (x = 1 (**1**) and 2 (**2**)), L_2 = $SiMe_2(\eta^5$-$C_5H_4)_2$ (x = 1 (**3**) and 2 (**4**)), and Ar′ = 2,6-$(CHMe_2)_2C_6H_3$ were prepared by the reaction of corresponding titanocene dichloride with LiOAr′ and characterized by spectroscopic methods and compound **3** by single crystal X-ray diffraction analysis. The bulky aryloxy ligand in **1** and **3** exerts a hindered rotation around the Ti–O bond on the ^{1}H NMR time scale, resulting in its dynamic behavior in $CDCl_3$ solution. Variable temperature NMR measurements proved the rotation barrier in **3** ($\Delta G^{\ddagger}_{298}$ = 13.9 ± 0.3 kcal/mol) to be lower than that in **1** ($\Delta G^{\ddagger}_{298}$ = 14.7 ± 0.2 kcal/mol) as a consequence of the more open titanocene shell in the *ansa*-structure of **3**. The catalytic behavior of complexes **1**–**4**, $[(\eta^5$-$C_5H_5)_2TiCl_2]$ and $[\{SiMe_2(\eta^5$-$C_5H_4)_2\}TiCl_2]$, was examined in dehydrocoupling polymerization of phenylsilane under comparable conditions, showing a remarkable higher activity for the titanocene complexes with regards to the *ansa*-titanocene ones. The order of catalytic activities **2** ~ **1** > $[(\eta^5$-$C_5H_5)_2TiCl_2]$ >> $[\{SiMe_2(\eta^5$-$C_5H_4)_2\}TiCl_2]$ ~ **3** ~ **4** reveals the aryloxy ligands to have an enhancing effect on activity in the titanocene series.

Keywords: Titanium; Metallocenes; Polymerizations; Silicon; Titanocene complexes; Dehydrocoupling; Polysilanes; Dynamic NMR spectroscopy; X-ray diffraction.

doi:10.1135/cccc2010133

Peculiar properties of polysilanes due to their σ-electron delocalization conjugation have been applied in design of new ceramic, semiconductor, photoresistive and nonlinear optic materials[1,2]. The preparation of polysilanes can be performed by two major methods – the Wurtz coupling of halosilanes and the dehydrocoupling of hydrosilanes catalyzed by transition metal complexes, the latter being known since the mid eighties[3]. In addition to late transition metal complexes (e.g. Wilkinson's catalyst $[(Ph_3P)_3RhCl])$[4], the group 4 metallocenes were found to be the most effective catalysts, as reviewed several times[5–7].

The main feature of the latter catalysts is the presence of a metal–ligand σ-bond which can react with the hydrosilane to form an active catalytic species participating in a catalytic dehydrocoupling cycle. Although not experimentally proved a metallocene hydride species is considered to initiate the dehydrocoupling via a σ-bond metathesis mechanism[8]. The catalysts reacting readily with hydrosilanes have been obtained *in situ* by mixing metallocene dichloride with alkylating/hydrogenating agents, e.g., $[Cp'_2MCl_2]$/2 eq. BuLi (where Cp′ = η^5-C_5H_5 and M is mainly Zr)[9–11], $[Me_2E(C_5Me_4)_2MCl_2]$/2 eq. BuLi (where E = C, Si and M = Ti, Zr, Hf)[12,13], and $[Cp'_2MCl_2]$/$NaAlH_2(OC_2H_4OCH_3)_2$ (where Cp′ = η^5-C_5H_5, η^5-C_5Me_5 M = Ti, Zr, Hf)[14,15]. These were widely used to obtain oligo-/polysilanes, however, they were unsuitable for the dehydrocoupling mechanism investigations.

Well-defined catalytic complexes $[Cp'_2MMe_2]$ (where Cp′ denotes mainly η^5-C_5H_5 ligand and M = Ti or Zr) bearing a highly reactive metal–carbon bond were introduced by Harrod et al.[3,16], and the structure of several titanocene silyl hydride complexes was elucidated. These complexes were apparently by-products or products of the catalyst deactivation, however[17,18]. Interestingly, titanium(II) complexes $[Cp'_2M(\eta^2$-BTMSA)] (where M = Ti, Zr and BTMSA = bis(trimethylsilyl)acetylene) were also shown to catalyze the dehydrocoupling of primary and secondary silanes[19,20].

In mid nineties, the air stable single-component catalyst precursors $[Cp_2Ti(OAr)_2]$ (where Ar = 4-XC_6H_4 and X= H, MeO, Cl, CN, Me) were reported to catalyze the silane dehydrocoupling although requiring higher reaction temperatures[21,22]. Shortly afterwards, the dehydrocoupling catalytic activity was recognized for $[(\eta^5$-$C_5H_5)_2MF_2]$ complexes (M = Ti, Zr)[23] followed by a family of metallocene pseudohalide complexes of general formula $[(\eta^5$-$C_5H_5)_2MY_2]$ (M = Ti, Zr, Hf and Y = F, OPh, NMe_2)[24]. Their activation was suggested to proceed via an initial removal of the electronegative element from the Ti–Y bond by the excess of silane followed by the formation of a Ti–H or Ti–Si bond.

Here we report the preparation, characterization and reactivity of titanocene derivatives of general formula $L_2TiCl_{2-x}(OAr')_x$ where L = η^5-C_5H_5 (x = 1 (**1**) and 2 (**2**)), L_2 = $SiMe_2(\eta^5$-$C_5H_4)_2$ (x = 1 (**3**) and 2 (**4**)), and Ar′ = 2,6-$(CHMe_2)_2C_6H_3$. Furthermore, the phenylsilane polymerization catalysed by **1**–**4**, and the parent $[(\eta^5$-$C_5H_5)_2TiCl_2]$ and $[\{SiMe_2(\eta^5$-$C_5H_4)_2\}TiCl_2]$ is described.

RESULTS AND DISCUSSION

Precatalyst Synthesis and Characterization

Complexes **1**–**4** were prepared by the reaction of appropriate titanocene dichloride with lithium 2,6-bis(isopropyl)phenoxide. The reaction of $[(\eta^5$-$C_5H_5)_2TiCl_2]$ with two equivalents of lithium 2,6-bis(isopropyl)phenoxide in boiling THF afforded a mixture of dark red titanocene aryloxychloro complex **1** and orange titanocene bis(aryloxy) complex **2** in a roughly 2:1 ratio (Scheme 1). The synthesis was not further optimized due to an easy separation of both complexes by fractional crystallization from hexane. Complex **1** was previously prepared by reacting $[(\eta^5$-$C_5H_5)_2TiCl_2]$ with one equivalent of 2,6-bis(isopropyl)phenol in the presence of NEt_3 as an organic base[25].

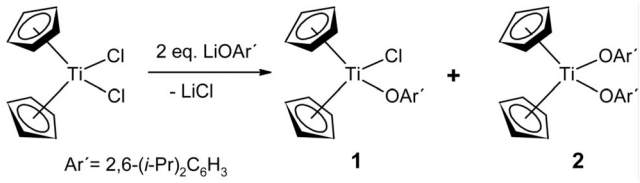

SCHEME 1

The reaction of *ansa*-titanocene dichloride $[\{SiMe_2(\eta^5$-$C_5H_4)_2\}TiCl_2]$ with either 1 or 2 equivalents of lithium 2,6-bis(isopropyl)phenoxide led only to the corresponding *ansa*-titanocene aryloxychloro complex **3** (Scheme 2). The *ansa*-titanocene bis(aryloxy) complex **4** was therefore prepared by reacting **3** with a 10-fold molar excess of lithium 2,6-bis(isopropyl)phenoxide

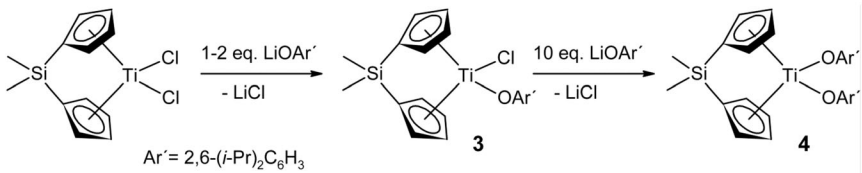

SCHEME 2

(Scheme 2). Even so, **4** was obtained in only moderate yield due to its difficult separation from similarly soluble lithium 2,6-bis(isopropyl)phenoxide tetrahydrofuran solvate (see Experimental).

Complexes **1**–**4** were characterized by standard spectroscopic methods. The ^{1}H and ^{13}C NMR spectra of **2** and **4** showed rather unsurprising sets of signals due to its C_{2v} molecular symmetry. The aryloxy ligands showed a similar signal pattern for both species. The *iso*-propyl group displayed a CH**Me**$_2$ doublet at 2.27 ppm (for both complexes) and a C**H**Me$_2$ septuplet centred at 3.32 ppm for **2** and 3.42 ppm for **4**. The quaternary aromatic carbon bearing the oxygen atom showed the δ_C signal at 168.36 ppm for **2** and 168.72 ppm for **4**. The reported values exhibit a considerable downfield shift (≈18 ppm) in comparison with the free aryloxy ligand as a consequence of the oxygen bonded to the titanium centre. A similar downfield shift of the quaternary aryloxy carbon signal in titanocene chloroaryloxy and titanocene bis(aryloxy) complexes was recently reported by Lang et al.[26]. $CDCl_3$ solutions of complexes **1** and **3** showed a dynamic behavior on the ^{1}H NMR time scale (see below).

The EI-MS spectra of **1**–**4** displayed molecular ions of rather low intensity, and further fragmentation depended on the metallocene framework. The *ansa*-titanocene complexes were losing preferentially the bulky aryloxy ligand giving base peaks *m/z* 269 $[M - OAr]^+$ for **3** and 411 $[M - OAr]^+$ for **4**, and the common $[SiMe_2(C_5H_4)_2]^+$ ion (*m/z* 234) in abundances 26 and 75%, respectively. On the other side, in addition to the aryloxy ligand (*m/z* 212 $[M - OAr]^+$ for **1** and 355 $[M - OAr]^+$ for **2**) titanocene complexes were losing the C_5H_5 ligand giving rise to base peaks *m/z* 324 $[M - C_5H_5]^+$ for **1** and 467 $[M - C_5H_5]^+$ for **2**. The results are consistent with a higher robustness of the *ansa*-system in comparison with the unbridged system[27].

IR spectra revealed the presence of η^5-C_5H_5 and $SiMe_2(\eta^5$-$C_5H_4)_2$ ligands, as obtained for $[(\eta^5$-$C_5H_5)_2TiCl_2]$ and $[\{SiMe_2(\eta^5$-$C_5H_4)_2\}TiCl_2]$, and sets of absorption bands due to 2,6-bis(isopropyl)phenoxide which were varying negligibly for **1**–**4**. The C–O valence vibration displays a strong absorption band in the range 1230–1260 cm^{-1} while the Ti–O valence vibration of medium intensity could be observable in the range 400–600 cm^{-1}.

*^{1}H NMR Study of Dynamic Behavior of Complexes **3** and **1***

Variable temperature measurements of $CDCl_3$ solutions of **1** and **3** in the temperature range from –40 to 40 °C (Fig. 1) revealed the dynamic behavior of the aryloxy ligand in **1** and **3** on the ^{1}H NMR time scale. At –40 °C, a frozen movement of the aryloxy ligand in **3** results in resolution of iso-

propyl signals as two septuplets centred at δ_H 2.93 and 3.37 ppm for methine protons and two doublets centred at δ_H 1.09 and 1.29 ppm for methyl groups. The methyl group signals coalesce at about 20 °C. Line fitting analysis performed by WINDNMR program[28] yielded the thermodynamic parameters $\Delta H^{\ddagger}$ = 11.0 ± 0.2 kcal/mol, $\Delta S^{\ddagger}$ = –9.6 ± 0.4 cal/K mol and standard free energy of activation $\Delta G^{\ddagger}_{298}$ = 13.9 ± 0.3 kcal/mol.

The hindered rotation of 2,6-bis(isopropyl)phenoxide group in the toluene-d_8 solution of **1** was noticed previously, however, without any further evaluation[25]. Here, ^{1}H NMR spectra of solution of **1** in $CDCl_3$ in the temperature range from –40 to 50 °C showed a coalescence of aryloxy methyl groups at 37 °C. Line fitting of signals by WINDNMR program was performed in the temperature range from –10 to 50 °C, and analysis of the data obtained gave the thermodynamic parameters $\Delta H^{\ddagger}$ = 11.3 ± 0.1 kcal/mol, $\Delta S^{\ddagger}$ = –11.2 ± 0.6 cal/K mol and standard free energy of activation $\Delta G^{\ddagger}_{298}$ = 14.7 ± 0.2 kcal/mol.

A discernibly lower $\Delta G^{\ddagger}_{298}$ value for **3** is consistent with the expected lower rotation barrier of the aryloxy ligand in the more opened *ansa*-titanocene shell. A similar lowering of rotational barrier of σ-ligand by

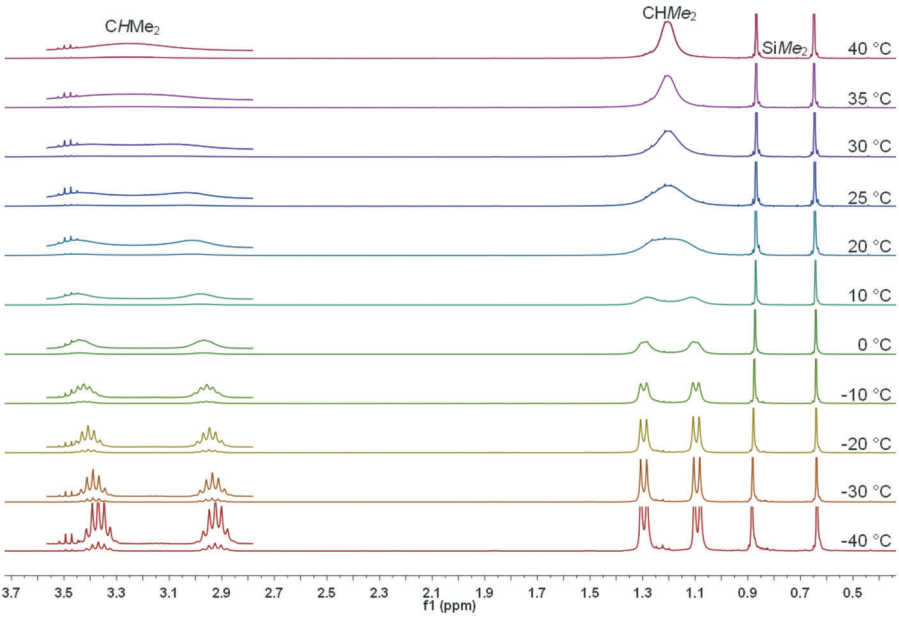

FIG. 1
Variable temperature ^{1}H NMR spectra of **3** in $CDCl_3$ measured in the temperature range from –40 to 40 °C

incorporation of $SiMe_2$ bridge between cyclopentadienyl rings was observed in zirconocene diphenyl complexes $[(\eta^5\text{-}C_5Me_5)_2ZrPh_2]$ ($\Delta G^{\ddagger}_{298}$ = 17.5 kcal/mol) and $[\{SiMe_2(\eta^5\text{-}C_5Me_4)_2\}ZrPh_2]$ ($\Delta G^{\ddagger}_{298}$ = 13.9 kcal/mol)[29].

*Reactivity of Complexes **2** and **3***

All prepared complexes are moderately stable in solid state if left on air for several hours; nevertheless, they are prone to hydrolysis in solution. The hydrolysis of **2** in $CDCl_3$ in the presence of excess of water was followed by ^{1}H NMR spectra. Surprisingly enough, after ca. 3 h, a new titanium complex was formed with the liberation of cyclopentadiene and 2,6-bis(isopropyl)phenol in a molar ratio ca. 1:2:2. The titanium complex contained one cyclopentadienyl ring (C_5H_5 at 6.16 ppm) and one OAr' ligand (doublet centred at δ_H 1.27 ppm for CH**Me**$_2$; septuplet centred at δ_H 3.31 ppm for C**H**Me_2), their presence in one complex was supported by 1D NOESY measurement. Judging from its composition it can form cyclic titanoxane $[(CpOAr'TiO)_n]$ complexes possessing Ti–O–Ti–O frameworks. The crystal structure of a similar propargyltitaniumoxy trimer was reported recently[30] and various titanoxane complexes were reviewed. The hydrolytic product was not isolated as it was further hydrolyzed to give a mixture of products.

To establish the relative stability of Cp–Ti and Ar'O–Ti bond against a strong Lewis acid, compound **3** was reacted with excess $TiCl_4$. The addition of $TiCl_4$ to the toluene solution of **3** resulted in precipitation of a brown solid. This was isolated and identified by ^{1}H and ^{13}C NMR spectroscopy to be $[\{SiMe_2(\eta^5\text{-}C_5H_4)_2\}TiCl_2]$. Its nearly quantitative formation means that the synproportionation reactions giving the dinuclear titanium complex $[Cl_3Ti(\eta^5\text{-}C_5H_4)SiMe_2(\eta^5\text{-}C_5H_4)Ti\{OC_6H_3\text{-}2,6\text{-}(CHMe_2)_2\}Cl_2]$ and/or $[SiMe_2\{(\eta^5\text{-}C_5H_4)TiCl_3\}_2]$[31] do not proceed under mild conditions. The ^{1}H and ^{13}C NMR analyses of the residue after evaporating the mother liquor in vacuum revealed a small amount of $[\{SiMe_2(\eta^5\text{-}C_5H_4)_2\}TiCl_2]$, while $[Ti\{OC_6H_3\text{-}2,6\text{-}(CHMe_2)_2\}Cl_3]$ and $[Ti\{OC_6H_3\text{-}2,6\text{-}(CHMe_2)_2\}_2Cl_2]$ were found in a molar ratio ca. 2:1. This can be accounted for the exclusive cleavage of the Ti–O bond in **3** with $TiCl_4$ forming an equimolar mixture of $[\{SiMe_2(\eta^5\text{-}C_5H_4)_2\}TiCl_2]$ and $[Ti\{OC_6H_3\text{-}2,6\text{-}(CHMe_2)_2\}Cl_3]$ where the latter complex is known to partially disproportionate in $CDCl_3$ solution into a mixture of $[Ti\{OC_6H_3\text{-}2,6\text{-}(CHMe_2)_2\}_2Cl_2]$ and $TiCl_4$ [32].

*Molecular Structure of **3***

The *ansa*-compound **3** crystallized with a triclinic lattice (space group *P*-1) having one formula unit located in the asymmetric part of the unit cell. The central titanium atom has a distorted tetrahedral coordination environment consisting of two cyclopentadienyl, one chlorine atom and one aryloxy group (Fig. 2). The distortion around the metal is the consequence of the unequal steric demands of the individual ligands. A notable molecular feature is the twisting of the aryloxy group towards one of the cyclopentadienyl ligands, demonstrating the effort of the oxygen atom trying to achieve a pseudotetrahedral arrangement in an attempt to minimize the repulsion between its valence electron pairs. The molecular structure is rather unexceptional in other respects and all geometrical parameters appear in the expected range. Selected bond lengths and angles are listed in Table I.

The molecular parameters of **3** are comparable with those of the parent dichloride [{$SiMe_2(\eta^5\text{-}C_5H_4)_2$}$TiCl_2$]. Although there were two polymorphs deposited in the Cambridge Structural Database[33,34], their molecular parameters were very alike. Thus Ti1–Cl(1) is 2.3699(4) Å for **3**, and 2.361 [33] and 2.356 Å [34] for [{$SiMe_2(\eta^5\text{-}C_5H_4)_2$}$TiCl_2$], respectively; Ti1–Cg are 2.1059(6) and 2.0752(6) Å for **3**, and 2.078 Å [33] and 2.075 Å [34] for [{$SiMe_2(\eta^5\text{-}C_5H_4)_2$}-$TiCl_2$], respectively; Cg(1)–Ti–Cg(2) is 128.57(3)° for **3**, and 128.87 [33] and 128.72° [34] for [{$SiMe_2(\eta^5\text{-}C_5H_4)_2$}$TiCl_2$], respectively.

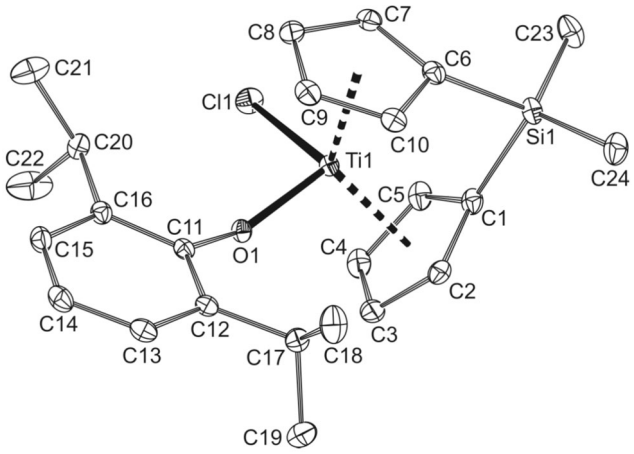

FIG. 2
PLATON drawing of compound **3** with the atom labelling scheme. Thermal motion ellipsoids are drawn at the 30% probability level. Hydrogen atoms are omitted for clarity

The parent complex in both solid-state structures had only one half of the molecule located in the asymmetric part of the unit cells; the symmetrically dependent part was generated applying the crystallographic two-fold axes in both cases. This is in contrast with the case of **3**, which becomes of lower symmetry upon substitution of the chloride ligand for the aryloxy one.

TABLE I
Selected bond lengths (in Å) and angles (in °) for **3**

Bond	Length, Å	Bond	Angle, °
Ti(1)–O(1)	1.8562(8)	Cg(1)–Ti(1)–Cg(2)	128.57(3)
Ti(1)–Cl(1)	2.3699(4)	O(1)–Ti(1)–Cl(1)	97.99(3)
Ti(1)–Cg(1)	2.1059(6)	Cg(1)–Ti(1)–Cl(1)	103.36(2)
Ti(1)–Cg(2)	2.0752(6)	Cg(1)–Ti(1)–O(1)	108.20(3)
C(11)–O(1)	1.3540(14)	Cg(2)–Ti(1)–Cl(1)	105.70(2)
C(1)–Si(1)	1.8682(13)	Cg(2)–Ti(1)–O(1)	108.61(3)
C(6)–Si(1)	1.8680(13)	C(11)–O(1)–Ti(1)	152.66(8)
		C(1)–Si(1)–C(6)	91.65(5)
		φ[a]	55.63(5)

[a] Dihedral angle between the least-squares planes of C(1–5) and C(6–10) cyclopentadienyl rings.

*DFT Calculation of Aryloxy Ligand Rotation in **3***

The mechanism and energy barrier of the aryloxy ligand rotation has been investigated by DFT computations of **3**. A full geometry optimization of the molecule yielded an arrangement virtually identical to that obtained from the X-ray diffraction experiment. The notable twisting of the aryloxy ligand towards one of the cyclopentadienyls was retained. According to natural bonding orbitals results[35], the Ti–O bond in **3** is dominantly ionic and is thus free to rotate along the interconnection axis. Further DFT studies were aimed at finding an energy maximum on the potential hypersurface by rotating the aryloxy ligand stepwise around the Ti–O bond. These geometries were studied by freezing the C(24)–Si(1)–C(11)–C(12) dihedral angle while leaving all other parameters free to optimize. An energy maximum was obtained at the dihedral angle 90°; the Ti(1)–O(1)–C(11) angle became 173.67° as a consequence of the increased repulsion between the ligands. The en-

ergy barrier computed at the BPW91/6-31G(d,p) theory level was 11.23 kcal/mol, which is close to the experimentally obtained value (vide supra) $\Delta H^{\ddagger}$ = 11.0 ± 0.2 kcal/mol.The correctness of geometry optimization of the conformer with the aryloxy group rotated has been verified by its computed infrared spectrum which contained no vibrations with imaginary frequencies.

*Dehydropolymerization of Phenylsilane Catalyzed by **1–4**, [(η^5-C_5H_5)$_2$$TiCl_2$] and [{$SiMe_2$($\eta^5$-$C_5H_4$)$_2$}$TiCl_2$]*

Reaction conditions and results of phenylsilane dehydrocoupling polymerization catalyzed by **1–4**, [(η^5-C_5H_5)$_2$$TiCl_2$] and [{$SiMe_2$($\eta^5$-$C_5H_4$)$_2$}$TiCl_2$], as well as characterization of the resulting polysilanes by GPC-MALLS are summarized in Table II. Similarly to the previously published [(η^5-C_5H_5)$_2$-

TABLE II
Polymerization of phenylsilane catalyzed by **1–4**, [(η^5-C_5H_5)$_2$$TiCl_2$] = ($Cp_2TiCl_2$) and [{$SiMe_2$($\eta^5$-$C_5H_4$)$_2$}$TiCl_2$] = ($SiCp_2TiCl_2$)[a]

Entry	Catal.	Catal. mole %	Temp. inic. °C	Temp. polym. °C	Conv. %	M_w (M_w/M_n)[b] kg/mol	LMW[c] %
1	**1**	0.10	110	110	94	1.36 (1.25)	(>17)
2	**2**	0.10	95	25	96	2.19 (1.50)	21
3	**2**	0.10	100	25	93	1.41 (1.33)	16
4	**2**	0.10	100	105	96	2.68 (1.52)	22
5[d]	**2**	0.05	100	25	66	0.53 (1.18)	n.d.
6	**2**	0.05	100	50	98	1.99 (1.44)	24
7	**2**	0.05	100	100	98	2.78 (1.59)	14
8	**3**	0.10	130	130	34	0.43 (1.15)	n.d.
9	**4**	0.10	130	130	35	2.09 (2.03)	n.d.
10	Cp_2TiCl_2	0.10	130	130	77	0.77 (1.17)	n.d.
11	Cp_2TiCl_2	0.20	130	130	88	1.29 (1.34)	n.d.
12	$SiCp_2TiCl_2$	0.10	130	130	38	Si_2–Si_5[e]	n.d.

[a] Reaction conditions: time 15 h, $n(PhSiH_3)$ = 15 mmol. [b] Determined by GPC-MALLS. [c] Low molecular weight fraction (composed mostly of Si_5–Si_6 cyclics) as determined by GPC-MALLS. [d] Polymerization in mixture silane/toluene 50/50 (v/v). [e] Oligomers up to pentamers as determined by ^{29}Si NMR.

$TiOPh_2$] complex[22], heating of complexes in neat phenylsilane is required to induce dehydrocoupling. The temperature at which the dehydrocoupling starts (indicated by an intense gas evolution) increases in the order: 50 °C for [$(\eta^5$-$C_5H_5)_2TiOPh_2$][22], 95–100 °C for **2**, 110 °C for **1**, and 130 °C for **3**, **4** [$(\eta^5$-$C_5H_5)_2TiCl_2$] and [{$SiMe_2(\eta^5$-$C_5H_4)_2$}$TiCl_2$]. Furthermore, the catalytical activity decreases in the order **2** ~ **1** > [$(\eta^5$-$C_5H_5)_2TiCl_2$] >> [{$SiMe_2(\eta^5$-$C_5H_4)_2$}$TiCl_2$] ~ **3** ~ **4**; showing that catalyst **2**, which could be activated at lowest temperature is the most convenient one.

GPC-MALLS analysis of polysilanes prepared with **1**, **2** and **4** showed a bimodal molecular weight distribution (M_w in the range 1360–2800 g/mol) with a lower molecular weight (LMW – see note in experimental section) fraction in the range 14–22 wt%, whereas complex [$(\eta^5$-$C_5H_5)_2TiCl_2$] produced rather low oligomers with M_w up to 1300 g/mol. The lowest M_w were found for oligosilanes prepared by complexes **3** and [{$SiMe_2(\eta^5$-$C_5H_4)_2$}$TiCl_2$]. In the latter case, the catalyst produced only linear oligomers up to pentamers as was evidenced by comparison of measured oligosilane δ_{Si} with the literature data[36].

As the dehydrocoupling process is influenced by reaction conditions[8,11,37], the effect of catalyst loading, temperature and toluene as a reaction medium was investigated with the most active complex **2**. The catalyst loading could be effectively reduced from 0.10 (entry 4) to 0.05 mole % (entry 7) without any effect on phenylsilane conversion, and the obtained polysilanes had almost identical molecular weight distributions. At higher temperature of polymerization (100 °C), polysilanes with higher molecular weight are produced (M_w = 2680 g/mol for entry 4) in comparison to polysilane prepared at room temperature (M_w = 1410 g/mol for entry 3), whereas LMW content remained similar for both entries. The dilution of polymerization feed with toluene leads to a decrease in reaction rate as indicated by the drop of monomer conversion and production of oligomers only (compare entries 3 and 5). The lowering of M_w value by phenylsilane polymerization in the presence of solvent was established previously[38,39].

The polysilane obtained from entry 2 was also analysed by means of ^{29}Si NMR spectroscopy. The ^{29}Si {^{1}H} INEPT experiment based on $^1J(^{29}Si$-$^1H)$ ~ 200 Hz polarization transfer showed similar results as the published ^{29}Si {^{1}H} DEPT experiments[40]. However, the standard ^{29}Si {^{1}H} NMR measurement revealed additional signals in the range from –68 to –80 ppm. The silicon atoms providing these resonances bear only phenyl groups and no hydrogen bonded directly. This fact was further proved by ^{29}Si {^{1}H} INEPT experiment based on $^3J(^{29}Si$-C-C-$^1H)$ ~ 7 Hz polarization transfer solely from the phenyl moieties (Fig. 3). These signals indicate redistribution of phenyl

groups at the silicon atom, leading to a formation of Ph_2Si unit, as a competing reaction to dehydrocoupling. Formation of phenylsilane oligomers with Ph_2Si unit is rather rare in polymerization catalyzed by group 4 complexes. The only known example is dealing with early stage phenylsilane polymerization catalyzed by $[(\eta^5\text{-}C_5H_5)HfCl_2]$/2 eq. BuLi system at higher temperatures[9].

On the other side, the substituent redistribution of alkyl and arylsilanes is a typical competing reaction to dehydrocoupling when catalysis by late transition metal complexes (e.g. $[(Ph_3P)_3RhCl]$) is employed[4,41,42].

EPR Investigations

The beginning of dehydrocoupling polymerizations initiated by titanocene complexes **1**, **2** and $[(\eta^5\text{-}C_5H_5)_2TiCl_2]$ is characterized, besides hydrogen evolution, by an intense color change of the reaction mixture changing from orange to deep green. This color apparently indicates the presence of Ti(III) complexes, which are proposed to be involved in a dehydrocoupling catalytic cycle. The formation and decay of paramagnetic species during the dehydrocoupling reaction was followed by means of EPR.

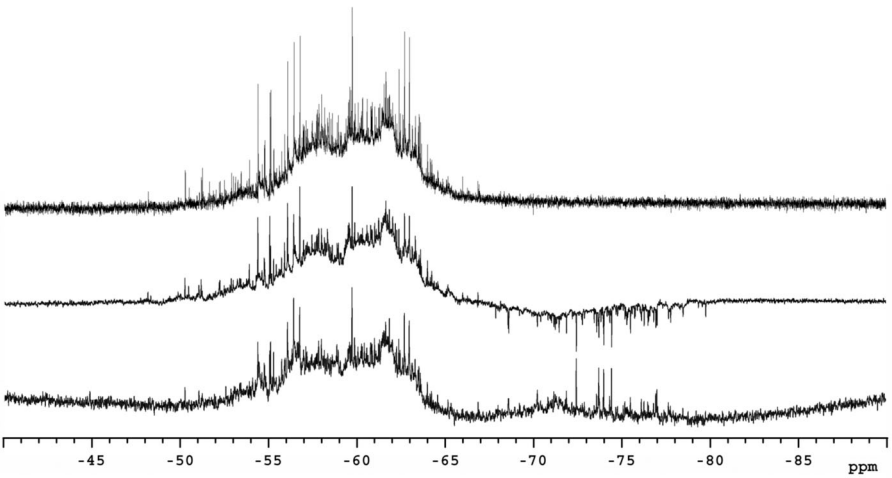

FIG. 3
^{29}Si NMR spectra of polysilane obtained from entry 2. The ^{29}Si $\{^1H\}$ INEPT experiment based on $^1J(^{29}Si\text{-}^1H) \sim 200$ Hz (top), $^3J(^{29}Si\text{-}C\text{-}C\text{-}^1H) \sim 7$ Hz polarization transfer (middle) and standard ^{29}Si $\{^1H\}$ NMR measurement (bottom)

The EPR spectra obtained upon warming of titanium precatalyst (**1**, **2** or $[(\eta^5\text{-}C_5H_5)_2\}TiCl_2]$) with neat phenylsilane (at Ti/$PhSiH_3$ molar ratio 1/1000) are characterized by the presence of an intense narrow singlet signal at g = 1.977(3) (ΔH = 3.8 G) having a recognizable hyperfine coupling to ^{47}Ti (I = 5/2) and ^{49}Ti (I = 7/2) nuclei with a_{Ti} = 4.6(1) G. This signal, albeit in a low intensity, was also detected immediately after admixing **1** with 1000 eq. of $PhSiH_3$ at room temperature, at the time when no visual indication of reaction could be detected. The signal intensity increased slowly with time, reached the maximum upon warming the mixture to 110 °C and then slowly ceased with a concomitant arising of a new broad (ΔH ~ 80 G) signal at the same g-value. A similar evolution and decay of the sharp EPR signal was also found for **2** and $[(\eta^5\text{-}C_5H_5)_2\}TiCl_2]$. A broad singlet signal at g = 1.9778 was previously observed and assigned to decomposition products of titanocene(III) silyl species[17,43]. In the present case, it is not clear, if the signal observed by us corresponds to a Ti(III) species involved in dehydrocoupling cycle or to a decomposition product.

Surprisingly, no evidence for the presence of $[\{(\eta^5\text{-}C_5H_5)_2TiH\}_2(\mu\text{-}H)]$ species isolated from $[(\eta^5\text{-}C_5H_5)_2TiMe_2]$/2 eq. $PhSiH_3$ system[3,17] or detected in $[(\eta^5\text{-}C_5H_5)_2TiF_2]$/2 eq. $PhSiH_3$ system[23], was found. However, the literature data were dealing with high Ti/silane ratio and toluene used as a solvent. It could be assumed, that the initially formed titanium hydrido species smoothly react with Si–H bonds to produce other titanium species when a large excess of phenylsilane is applied.

DISCUSSION

The above experiments showed a substantially lower efficiency of *ansa*-titanocene precatalysts in comparison to titanocene ones. Similar trend in reactivity was observed when two component catalytic systems $[(\eta^5\text{-}C_5H_5)_2MCl_2]$/2 eq. BuLi (where M = Ti, Zr, Hf) and $[Me_2E(\eta^5\text{-}C_5H_5)_2MCl_2]$/2 eq. BuLi (where E = C, Si and M = Ti, Zr, Hf) were compared[12,13]. The obtained results are rather unexpected on the basis of known properties of both complex types and suggestion of Ti(III) hydride species as a true catalytic species. One could expect better activities for *ansa*-titanocene complexes due to their electronic and steric properties.

First, the *ansa*-complex $[\{SiMe_2(\eta^5\text{-}C_5H_4)_2\}TiCl_2]$ ($E^0{}_1$ = –1.283 V) has a lower first reduction potential than $[(\eta^5\text{-}C_5H_5)_2TiCl_2]$ ($E^0{}_1$ = –1.313 V)[44], that implies its easier reduction to Ti(III) as a prerequisite for the formation of catalytically active species. Second, the open shell around the active titanium site in *ansa*-titanocenes should provide more space for the incoming

silane in comparison with the titanocene. The steric factor was suggested to be responsible for a generally much lower polymerization capability of bulkier Ph_2SiH_2 compared to $PhSiH_3$ [10].

In the absence of experimental evidence the answer for the low activity of the *ansa*-complexes can be sought from the different behavior of low valent *ansa*-titanocene in comparison to their unbridged equivalents. As it was shown by Brintzinger, the *ansa*-titanocene [{$(CH_2)_2(\eta^5\text{-}C_5H_4)_2$}$TiCl_2$] did not follow the reaction path known for their unbridged analogues, such as formation of Ti(III) hydride compound. These reactions are proposed to be blocked by the unavailability of a "free" *ansa*-titanocene species {Cp_2Ti} as an intermediate[45]. Similarly, the formation of {Cp_2Ti} intermediate was proposed as a prerequisite step in accelerating the generation of active dehydrocoupling species [Cp_2TiH] from [Cp_2TiY_2] precursor (where Y = Me [5] and Y = F, OPh, NMe_2 [24]). An alternative explanation for lower productivity of *ansa*-complexes was proposed by Corey and co-workers. They proposed a siphoning of the active species into inactive dimer facilitated by opening the coordination site in the *ansa*-framework[12,13].

CONCLUSION

The four new titanocene and *ansa*-titanocene complexes bearing bulky σ-bonded anionic 2,6-bis(isopropyl)phenoxide ligand were prepared and characterized by conventional spectroscopic methods (NMR, IR, EI-MS) and by X-ray diffraction analysis. The prepared complexes were found to be active catalysts in dehydrocoupling polymerization of phenylsilane. The metallocene ligand framework in the titanocene catalyst was found to be a predominant factor for the catalyst efficiency and selectivity. The titanocene complexes polymerize phenylsilane with a higher reactivity and to higher M_w than the *ansa*-titanocene complexes. In addition, the bis(aryloxy)titanocene exhibit a higher reactivity and produce polysilane with a higher M_w than the chloroaryloxy and the dichloro titanocene complexes.

EXPERIMENTAL

All reactions with moisture- and air-sensitive compounds were carried out under argon (99.998%) using standard Schlenk techniques. Solvents were dried, and freshly distilled prior to use. *n*-Butyllithium (1.6 M solution in hexane), 2,6-bis(isopropyl)phenol and titanocene dichloride were obtained from Aldrich and used as received. Phenylsilane was obtained from Fluka and dried by refluxing over $LiAlH_4$ prior to distillation. Florisil 60–100 mesh (Roth) was dried at 120 °C in vacuum for 13 h. [{$SiMe_2(\eta^5\text{-}C_5H_4)_2$}$TiCl_2$] was prepared according to

literature procedure[34]. Lithium 2,6-bis(isopropyl)phenoxide was prepared similarly as described in literature[46], except that hexane was used as a solvent to avoid the solvate formation. ^{1}H NMR (THF-d_8): 1.17 d, $^3J_{HH}$ = 6.9, 12 H (CH**Me**$_2$); 3.58 septuplet, $^3J_{HH}$ = 6.9, 2 H (C**H**Me$_2$); 6.32 t, $^3J_{HH}$ = 7.5, 1 H (C(4)H, C_6H_3); 6.80 d, $^3J_{HH}$ = 7.5, 2 H (C_6H_3).

^{1}H and ^{13}C NMR spectra were recorded on a Varian Mercury 300 spectrometer at 300.0 MHz and 75.4 MHz, respectively, in $CDCl_3$ solutions at 25 °C, or for temperature dependent experiments in the range from –40 to 50 °C. Chemical shifts (δ, ppm) are given relative to solvent signals (δ_H 7.26, δ_C 77.16); coupling constants are given in Hz. ^{29}Si NMR spectral measurements of polysilanes were performed on a Varian UNITY-500 spectrometer (operating at 499.9 MHz for ^{1}H and 99.3 MHz for ^{29}Si nucleus) in $(CD_3)_2CO$ solution at 20 °C. The standard ^{29}Si {^{1}H} NMR measurement were done with relaxation delay 58 s and acquisition time 2 s. The ^{29}Si {^{1}H} INEPT experiment was based on $^1J(^{29}Si\text{-}^1H)$ ~ 200 Hz polarization transfer (0.0025 ms) with the refocusing delay 0.0025 ms, relaxation delay 3 s and acquisition time 2 s. The ^{29}Si {^{1}H} INEPT experiment based on $^3J(^{29}Si\text{-}C\text{-}C\text{-}^1H)$ ~ 7 Hz had the polarization transfer 0.018 ms with the refocusing delay set to 0.038 ms (these values were optimized to provide maximum intensity), relaxation delay was 3 s and acquisition time 2 s. EI-MS spectra were obtained on a VG-7070E mass spectrometer at 70 eV. Crystalline samples in sealed capillaries were opened and inserted into the direct inlet under argon. IR spectra (ν, cm^{-1}) were taken in an air-protecting cuvette on a Nicolet Avatar FTIR spectrometer in the range 400–4000 cm^{-1}. KBr pellets were prepared in a glovebox Labmaster 130 (mBraun) under purified nitrogen. Melting points were measured on a Koffler block and were uncorrected. EPR spectra were measured on an ERS-220 spectrometer (Center for Production of Scientific Instruments, Academy of Sciences of G.D.R., Berlin, Germany) operated by a CU-3 unit (Magnettech, Berlin, Germany) in the X-band. *g*-Values were determined using an Mn^{2+} standard signal at g = 1.9860 (M_I = –1/2 line). Elemental analyses were carried out on a FLASH EA1112 CHN/O automatic elemental analyser (Thermo Scientific). Molar masses of polysilanes were determined on a Waters Breeze chromatographic system (Waters 2410 refractive index detector, Waters 1515 pump, Waters 717plus Autosampler, column heater) with RI detector operating at 880 nm and multi-angle laser light scattering miniDawn TREOS from Wyatt with laser wavelength 658 nm. Refractive index increments (dn/dc = 0.238–0.268 ml/g) were measured on-line on RI detector at 880 nm. Separation was performed on two 7.8 mm × 300 mm Polymer Laboratories Mixed C columns at 35 °C in THF at an elution rate of 1 ml/min. Sample concentrations were 3–5 mg/ml. Light scattering data were evaluated using Astra 5.3.2.15 software. The amount of LMW fraction was evaluated from the deconvolution of GPC chromatogram of respective polysilane. Although the LMW fraction is attributed mostly to cyclic products, GC-MS analysis of volatile fractions of polysilane obtained from entry 2 showed also presence of lower linear oligomers up to tetramers. Therefore the presence of linear oligomers should be also taken into account in LMW fraction.

Preparation of **1** and **2**

To a cold (–78 °C) suspension of $[(\eta^5\text{-}C_5H_5)_2TiCl_2]$ (0.76 g, 3.05 mmol) in THF (60 ml), solid lithium 2,6-bis(isopropyl)phenoxide (1.13 g, 6.14 mmol) was gradually added. The mixture was allowed to warm up to room temperature, then stirred for 13 days and evaporated to dryness afterwards. The obtained dark red waxy solid was extracted in 40 ml of hexane. Concentration of hexane solution to ca. 20 ml and its storing in fridge (5 °C) overnight pro-

duced dark red crystals of **1**. The crystals were isolated, washed by cold hexane (3 × 2 ml) and dried in vacuum. Yield 0.38 g (32%).

The mother liquor was combined with washings, and the solvent was partially evaporated in vacuum. Orange microcrystals of **2** precipitated out after one week standing. They were isolated, washed by cold hexane (2 ml) and dried in vacuum. Yield 0.22 g (14%).

[(η^5-C_5H_5)$_2$TiCl(OC_6H_3-2,6-iPr)] (**1**): M.p. 160 °C. ^{1}H NMR ($CDCl_3$, 238 K): 1.11 d, $^3J_{HH}$ = 6.9, 6 H (CH**Me**$_2$); 1.29 d, $^3J_{HH}$ = 6.6, 6 H (CH**Me**$_2$); 2.77 septuplet, $^3J_{HH}$ = 6.9, 1 H (C**H**Me$_2$); 3.39 septuplet, $^3J_{HH}$ = 6.6, 1 H (C**H**Me$_2$); 6.36 s, 10 H (C_5H_5); 6.90 t, $^3J_{HH}$ = 7.8, 1 H (C(4)H, C_6H_3); 7.06–7.14 m, 2 H (C_6H_3). ^{13}C {^{1}H} NMR ($CDCl_3$): 23.5, 24.3 (CH**Me**$_2$); 26.1 (**C**HMe$_2$); 117.6 (C_5H_5); 120.5 (C(4)H, C_6H_3); 123.2, 123.6 (C(3)H and C(5)H, C_6H_3); 166.1 (C(1)O, C_6H_3). IR (KBr): 3111 (w), 3093 (w), 3054 (w), 2961 (s), 2923 (m), 2865 (m), 1586 (vw), 1455 (m), 1429 (vs), 1381 (vw), 1359 (w), 1345 (vw), 1327 (vs), 1255 (s), 1205 (s), 1114 (m), 1095 (m), 1072 (vw), 1056 (vw), 1043 (vw), 1029 (w), 1013 (w), 934 (vw), 894 (m), 864 (m), 845 (m), 825 (s), 814 (vs), 793 (w), 750 (s), 704 (w), 698 (w), 669 (vw), 584 (vw). EI-MS, *m/z* (rel. abundance): 391 (12), 390 (9), 389 ($M^{\bullet+}$, 24), 354 ([M – Cl]$^+$, 7), 326 (7), 324 ([M – C_5H_5]$^+$, 19), 322 (13), 286 (13), 214 (41), 213 (23), 212 ([M – $OC_6H_3(CHMe_2)_2$]$^+$, 100), 211 (12), 210 (12), 177 ([M – $OC_6H_3(CHMe_2)_2$ – Cl]$^+$, 17), 149 (10), 147 ([(C_5H_5)TiCl]$^+$, 22). For $C_{22}H_{27}ClOTi$ (390.79) calculated: 67.61% C, 6.96% H; found: 67.49% C, 7.06% H.

Note: Elemental analysis, ^{1}H and ^{13}C NMR in toluene-d_8 were already published for **1** [25].

[(η^5-C_5H_5)$_2$Ti(OC_6H_3-2,6-iPr)$_2$] (**2**): M.p. 175 °C. ^{1}H NMR ($CDCl_3$): 1.27 d, $^3J_{HH}$ = 6.9, 24 H (CH**Me**$_2$); 3.32 septuplet, $^3J_{HH}$ = 6.9, 4 H (C**H**Me$_2$); 6.17 s, 10 H (C_5H_5); 6.92 t, $^3J_{HH}$ = 7.5, 2 H (C(4)H, C_6H_3); 7.11–7.18 m, 4 H (C_6H_3). ^{13}C {^{1}H} NMR ($CDCl_3$): 24.97 (CH**Me**$_2$); 26.13 (**C**HMe$_2$); 116.35 (C_5H_5); 120.13 (C(4)H, C_6H_3); 123.63 (C(3)H and C(5)H, C_6H_3); 136.52 (C(2) and C(6), C_6H_3); 168.36 (C(1)O, C_6H_3). IR (KBr): 3051 (m), 2963 (s), 2868 (m), 1587 (w), 1466(m), 1427 (vs), 1383 (w), 1359 (w), 1320 (s), 1249 (vs), 1237 (s), 1196 (vs), 1157 (w), 1116 (m), 1098 (m), 1043 (w), 1016 (m), 933 (vw), 885 (m), 853 (s), 809 (s), 793 (s), 753 (s), 693 (w), 568 (w). EI-MS, *m/z* (rel. abundance): 532 ($M^{\bullet+}$, 6), 469 (53), 468 (89), 467 ([M – C_5H_5]$^+$, 100), 466 (72), 465 (84), 357 (48), 356 (87), 355 ([M – $OC_6H_3(CHMe_2)_2$]$^+$, 99), 354 (52), 353 (61), 290 (21), 289 (30), 288 (85), 287 (87), 286 (29), 285 (29), 274 (31), 273 (30), 272 (22), 271 (26), 247 (79), 245 (29), 243 (32), 179 (31), 178 ([M – 2 ($OC_6H_3(CHMe_2)_2$)]$^+$, 82). For $C_{34}H_{44}O_2Ti$ (532.59) calculated: 76.67% C, 8.33% H; found: 76.83% C, 8.41% H.

Preparation of [{$SiMe_2$(η^5-C_5H_4)$_2$}TiCl(OC_6H_3-2,6-*i*Pr)] (**3**)

Method A. To a mixture of [{$SiMe_2$(η^5-C_5H_4)$_2$}$TiCl_2$] (0.81 g, 2.66 mmol) and lithium 2,6-bis(isopropyl)phenoxide (0.52 g, 2.83 mmol) hexane (80 ml) was transferred and the mixture was refluxed for 7 days. The resulting suspension was cooled to room temperature and filtered immediately from a grey precipitate. Red crystals were formed after standing of the filtrate at room temperature for several hours. The crystallization was completed by standing at –28 °C overnight. Crystals were isolated, washed with cold hexane (2 × 5 ml) and dried in vacuum. Yield 0.93 g (78%).

Method B. To a suspension of [{$SiMe_2$(η^5-C_5H_4)$_2$}$TiCl_2$] (0.26 g, 0.85 mmol) in THF (20 ml), the solution of lithium 2,6-bis(isopropyl)phenoxide (0.16 g, 0.87 mmol) in THF (20 ml) was added drop wise within 1 h. The mixture was stirred for 14 h and then evaporated to dryness. The product was extracted in hot hexane (25 ml) and the resulting red solution was cooled to room temperature and concentrated to ca. 7 ml. Red crystals which precipitated

after standing at room temperature for several hours were isolated, washed with hexane (2 × 1 ml) and dried in vacuum. The second crop of crystals was obtained by keeping mother liquor at 4 °C for several days. Combined yield 0.25 g (64%).

M.p. 162 °C. ^{1}H NMR ($CDCl_3$, 233 K): 0.64, 0.89 2 × s, 2 × 3 H ($SiMe_2$); 1.09 d, $^3J_{HH}$ = 7.2, 6 H (CH**Me**$_2$); 1.29 d, $^3J_{HH}$ = 6.6, 6 H (CH**Me**$_2$); 2.93 septuplet, $^3J_{HH}$ = 6.6, 1 H (C**H**Me_2); 3.37 septuplet, $^3J_{HH}$ = 7.2, 1 H (C**H**Me_2); 6.02–6.07 m, 1 H (C_5H_4); 6.08–6.23 m, 1 H (C_5H_4); 6.45–6.50 m, 1 H (C_5H_4); 6.66–6.72 m, 1 H (C_5H_4); 6.87 (t, $^3J_{HH}$ = 7.8, 1 H (C(4)H, C_6H_3); 7.01 m, 2 H (C_6H_3). ^{13}C {^{1}H} NMR ($CDCl_3$, 233 K): –6.55 ($SiMe_2$); –3.92 ($SiMe_2$); 23.48 (CH**Me**$_2$); 24.29 (CH**Me**$_2$); 25.45 (**C**HMe_2); 26.19 (**C**HMe_2); 109.69 (C_{ipso}, C_5H_4); 110.43 (CH, C_5H_4); 120.05 (C(4)H, C_6H_3); 123.13 (CH, C_5H_4); 123.25, 123.31 (C(3)H and C(5)H, C_6H_3); 126.15 (CH, C_5H_4); 132.42 (CH, C_5H_4); 133.56, 137.10 (C(2) and C(6), C_6H_3); 165.37 (C(1)O, C_6H_3). ^{29}Si {^{1}H} NMR ($CDCl_3$): –12.68 ($SiMe_2$). IR (KBr): 3114 (w), 3068 (w), 3054 (w), 3023 (w), 2967 (s), 2942 (s), 2863 (m), 1588 (vw), 1456 (w), 1434 (vs), 1402 (w), 1372 (w), 1359 (w), 1349 (vw), 1330 (vs), 1258 (vs), 1205 (vs), 1168 (m), 1109 (w), 1097 (w), 1076 (w), 1051 (m), 1039 (m), 937 (vw), 893 (s), 873 (s), 834 (vs), 810 (vs), 794 (vs), 753 (s), 704 (w), 681 (m), 669 (s), 624 (vw), 603 (w), 588 (w), 461 (w), 438 (vw), 411 (vw). EI-MS, *m/z* (rel. abundance): 448 (9), 447 (8), 446 ($M^{\bullet+}$, 17), 411 ([M – Cl]$^+$, 13), 409 (10), 272 (16), 271 (63), 270 (43), 269 ([M – $OC_6H_3(CHMe_2)_2$]$^+$, 100), 268 (18), 267 (17), 254 (11), 235 (8), 234 ([M – $OC_6H_3(CHMe_2)_2$ – Cl]$^+$, 26), 91 (11), 43 (22), 41 (23). For $C_{24}H_{31}ClOSiTi$ (446.93) calculated: 64.49% C, 6.99% H; found: 64.52% C, 6.93% H.

Preparation of [{$SiMe_2(\eta^5$-$C_5H_4)_2$}Ti(OC_6H_3-2,6-*i*Pr)$_2$] (**4**)

Lithium 2,6-bis(isopropyl)phenoxide (0.62 g, 3.37 mmol) was added to a solution of **3** (0.17 g, 0.38 mmol) in THF (15 ml) and the resulting red reaction mixture was heated to 55 °C for 5 days. Volatiles were evaporated in vacuum and the solid residue was extracted into hexane (20 ml). Concentration of the hexane solution to ca. 8 ml, followed by cooling to –78 °C for 4 h, resulted in precipitation of a yellow solid. The solid was identified as lithium 2,6-bis(isopropyl)phenoxide–tetrahydrofurane solvate on the basis of ^{1}H and ^{13}C NMR spectroscopy. The mother liquor was concentrated to ca. 4 ml and stored in a freezer (–35 °C). The orange microcrystals of **4** formed after several days have been isolated, washed by cold hexane and dried in vacuum. Yield 0.10 g (44%). M.p. 180–184 °C. ^{1}H NMR ($CDCl_3$): 0.77 s, 6 H ($SiMe_2$); 1.26 d, $^3J_{HH}$ = 6.9, 24 H (CH**Me**$_2$); 3.42 septuplet, $^3J_{HH}$ = 6.9, 4 H (C**H**Me_2); 5.76–5.80 pseudo t, 4 H (C_5H_4); 6.52–6.58 pseudo t, 4 H (C_5H_4); 6.91 t, $^3J_{HH}$ = 7.5, 2 H (C(4)H, C_6H_3); 7.01 d, $^3J_{HH}$ = 7.5, 4 H (C_6H_3). ^{13}C {^{1}H} NMR ($CDCl_3$): –5.17 ($SiMe_2$); 24.85 (CH**Me**$_2$); 26.06 (**C**HMe_2); 111.06 (C_{ipso}, C_5H_4); 112.89 (CH, C_5H_4); 120.24 (C(4), C_6H_3); 123.74 (C(3) and C(5), C_6H_3); 128.67 (CH, C_5H_4); 136.63 (C(2) and C(6), C_6H_3); 168.72 (C(1)O, C_6H_3). ^{29}Si {^{1}H} NMR ($CDCl_3$): –13.07 ($SiMe_2$). IR (KBr): 3071 (vw), 3053 (w), 3018 (vw), 2962 (vs), 2867 (m), 1587 (w), 1461 (m), 1428 (vs), 1381 (vw), 1359 (w), 1321 (s), 1253 (vs), 1239 (m), 1196 (s), 1157 (vw), 1116 (vw), 1098 (w), 1079 (vw), 1044 (m), 933 (vw), 907 (vw), 886 (w), 856 (m), 850 (s), 829 (m), 808 (m), 789 (w), 751 (s), 694 (w), 677 (vw), 664 (vw), 619 (vw), 571 (w), 460 (vw). EI-MS, *m/z* (rel. abundance): 588 ($M^{\bullet+}$, 6), 413 (34), 412 (72), 411 ([M – $(C_6H_3(C_3H_7)_2O)$]$^+$, 100), 410 (36), 409 (42), 407 (12), 288 (12), 236 (23), 235 (23), 234 ([M – 2 $(C_6H_3(C_3H_7)_2O)$]$^+$, 75), 233 (13), 135 (15), 107 (11), 91 (9), 43 ([C_3H_7]$^+$, 26), 41 (13). For $C_{36}H_{48}O_2SiTi$ (588.73) calculated: 73.44% C, 8.22% H; found: 73.69% C, 8.36% H.

Reaction of **3** with $TiCl_4$

An excess of $TiCl_4$ (0.5 ml, 4.50 mmol) was added to a solution of **3** (0.56 g, 1.25 mmol) in toluene (50 ml) under stirring at room temperature. The mixture changed its color from red-orange to deep red and a brown precipitate was immediately formed. The mixture was stirred for additional 2 h and then left standing at –28 °C overnight. The brown precipitate was isolated, washed with hexane (2 × 8 ml) and dried in vacuum. Yield 0.29 g (63%). The NMR analysis of the solid product proved that it was $[\{SiMe_2(\eta^5\text{-}C_5H_4)_2\}TiCl_2]$[34]. The deep red mother liquor was evaporated to dryness, re-dissolved in $CDCl_3$ and analysed by ^1H and ^{13}C NMR spectroscopy as a mixture $[Ti\{OC_6H_3\text{-}2,6\text{-}(CHMe_2)_2\}Cl_3]$ and $[Ti\{OC_6H_3\text{-}2,6\text{-}(CHMe_2)_2\}_2Cl_2]$ on the basis of literature data[32].

Phenylsilane Polymerization

The polymerizations of phenylsilane were performed in a Schlenk tube under inert atmosphere. An example of polymerization is given below for entry 2. Phenylsilane (1.62 g, 15.0 mmol) was added to solid **2** (0.008 g, 15 μmol), and the mixture was heated to 95 °C causing the color change to green and gas evolution. After 20 min, the mixture was cooled to room temperature and stirred for additional 15 h. Volatiles were evaporated in vacuum and the resulting green wax was dissolved in toluene. The toluene solution was filtered through a plug of Florisil (2 × 5 cm) and the solid phase was washed with toluene (20 ml). Combined toluene fractions were evaporated in vacuum to obtain poly(phenylsilane) as a slightly yellow wax. Yield 1.57 g (96%).

EPR Experiments

The EPR experiments were measured in an EPR tube connected directly to a Schlenk vessel. An appropriate amount of catalyst (15 μmol) was mixed with 1000 molar equivalents of $PhSiH_3$, and the mixture was heated until the color has begun to change to green and gas evolution has been observed (ca. 10 min for **1** at 110 °C, for **2** at 100 °C and for $[(\eta^5\text{-}C_5H_5)_2TiCl_2]$ at 130 °C). The mixture was cooled to room temperature, transferred to the EPR tube and measured at 22 °C.

X-ray Crystallography

Red crystals of **3** were grown from its hexane solution upon slow cooling. A suitable crystal for the X-ray single-crystal analysis was selected under a polarization microscope. Diffraction data were collected using a Nonius KappaCCD diffractometer at 150 K and were processed using the HKL program package[47]. The phase problem was solved by SIR-97 [48] and the structure was refined by least-squares using the SHELXL-97 [49] program. All heavy atoms were refined anisotropically. Hydrogen atoms were included in ideal positions and refined isotropically. Relevant crystallographic data are collected in Table III. CCDC 782470 contains the supplementary crystallographic data for this paper. These data can be obtained free of charge via www.ccdc.cam.ac.uk/conts/retrieving.html (or from the Cambridge Crystallographic Data Centre, 12, Union Road, Cambridge, CB2 1EZ, UK; fax: +44 1223 336033; or deposit@ccdc.cam.ac.uk).

DFT Studies

DFT computations have been carried out at the fermi cluster of the Computer Centre at the J. Heyrovský Institute of Physical Chemistry, Academy of Sciences of the Czech Republic, v.v.i., using Gaussian 03, revision E.01 [50]. The computations employed the BPW91 functional; the 6-31G(d,p) basis set was used for all atoms. After optimizing the solid-state structure with all molecular parameters free to optimize, the rotation maximum of the aryloxy group was searched by rotating the aromatic ring stepwise and repeating the geometry optimization step with the position of the aryloxy group frozen. Natural bond orbital analyses were done using the NBO 3.1 program integrated in Gaussian.

TABLE III
Crystal data and structure refinement for **3**

Empirical formula	$C_{24}H_{31}ClOSiTi$
Formula weight	446. 93 g/mol
Temperature	150(1) K
Wavelength	0.71073 Å
Crystal system, space group	Triclinic, *P*-1 (No. 2)
Unit cell dimensions	a = 9.48690(10) Å α = 78.8888(8)°
	b = 10.5429(2) Å β = 82.5883(10)°
	c = 11.8209(2) Å γ = 82.0360(9)°
Unit cell volume	1142.58(3) Å^3
Z, Calculated density	2, 1.299 g/cm^3
Absorption coefficient	0.556 mm^{-1}
F(000)	472
Crystal size	0.81 × 0.50 × 0.25 mm
θ range for data collection	1.77 to 27.50°
Limiting indices	$-12 \le h \le 12$, $-13 \le k \le 13$, $-15 \le l \le 15$
Reflections collected/unique	10333/5238 [R(int) = 0.0118]
Completeness to θ = 27.50°	99.7%
Max. and min. transmission	0.8735 and 0.6616
Refinement method	Full-matrix least-squares on F^2
Data/restrains/parameters	5238/0/259
Goodness-of-fit on F^2	1.042
Final R indices [$I > 2\sigma(I)$]	$R1$ = 0.0269, $wR2$ = 0.0690
R indices (all data)	$R1$ = 0.0296, $wR2$ = 0.0707
Largest diff. peak and hole	0.396 and –0.307 eÅ^{-3}

The financial support from the Czech Science Foundation (Project GA203/09/1574), Academy of Sciences of the Czech Republic (Project KAN100400701) and from the Ministry of Education, Youth and Sports of the Czech Republic (Projects MSM0021620857, MSM 6046137302 and LC06070) is gratefully acknowledged.

REFERENCES

1. West R.: *J. Organomet. Chem.* **1986**, *300*, 327.
2. Miller R. D., Michl J.: *Chem. Rev.* **1989**, *89*, 1359.
3. Samuel E., Harrod J. F.: *J. Am. Chem. Soc.* **1984**, *106*, 1859.
4. Rosenberg L., Kobus D. N.: *J. Organomet. Chem.* **2003**, *685*, 107.
5. Harrod J. F.: *Coord. Chem. Rev.* **2000**, *206–207*, 493.
6. Clark T. J., Lee K., Manners I.: *Chem. Eur. J.* **2006**, *12*, 8634.
7. Corey J. Y.: *Advances in Organometallic Chemistry*, Vol. 51, p. 1. Academic Press Inc., San Diego 2004.
8. Tilley T. D.: *Acc. Chem. Res.* **1993**, *26*, 22.
9. Corey J. Y., Zhu X. H.: *J. Organomet. Chem.* **1992**, *439*, 1.
10. Corey J. Y., Zhu X. H., Bedard T. C., Lange L. D.: *Organometallics* **1991**, *10*, 924.
11. Obora Y., Tanaka M.: *J. Organomet. Chem.* **2000**, *595*, 1.
12. Shaltout R. M., Corey J. Y., Rath N. P.: *J. Organomet. Chem.* **1995**, *503*, 205.
13. Shaltout R. M., Corey J. Y.: *Tetrahedron* **1995**, *51*, 4309.
14. Woo H. G., Kim S. Y., Han M. K., Cho E. J., Jung I. N.: *Organometallics* **1995**, *14*, 2415.
15. Woo H. G., Song S. J.: *Chem. Lett.* **1999**, 457.
16. Mu Y., Aitken C., Cote B., Harrod J. F., Samuel E.: *Can. J. Chem.-Rev. Can. Chim.* **1991**, *69*, 264.
17. Aitken C. T., Harrod J. F., Samuel E.: *J. Am. Chem. Soc.* **1986**, *108*, 4059.
18. Samuel E., Mu Y., Harrod J. F., Dromzee Y., Jeannin Y.: *J. Am. Chem. Soc.* **1990**, *112*, 3435.
19. Peulecke N., Thomas D., Baumann W., Fischer C., Rosenthal U.: *Tetrahedron Lett.* **1997**, *38*, 6655.
20. Lunzer F., Marschner C., Winkler B., Peulecke N., Baumann W., Rosenthal U.: *Monatsh. Chem.* **1999**, *130*, 215.
21. Corriu R. J. P., Enders M., Huille S., Moreau J. J. E.: *Chem. Mater.* **1994**, *6*, 15.
22. Bourg S., Corriu R. J. P., Enders M., Moreau J. J. E.: *Organometallics* **1995**, *14*, 564.
23. Lunzer F., Marschner C., Landgraf S.: *J. Organomet. Chem.* **1998**, *568*, 253.
24. Wang Q. Z., Corey J. Y.: *Can. J. Chem.-Rev. Can. Chim.* **2000**, *78*, 1434.
25. Firth A. V., Stewart J. C., Hoskin A. J., Douglas D. W.: *J. Organomet. Chem.* **1999**, *591*, 185.
26. Köcher S., Walfort B., Rheinwald G., Rüffer T., Lang H.: *J. Organomet. Chem.* **2008**, *693*, 3213.
27. Shapiro P. J.: *Coord. Chem. Rev.* **2002**, *231*, 67.
28. Reich H. J.: *WINDNMR; NMR Spectrum Calculations*. University of Wisconsin, Madison 2005.
29. Lee H., Bridgewater B. M., Parkin G.: *J. Chem. Soc., Dalton Trans.* **2000**, 4490.
30. Pinkas J., Gyepes R., Císařová I., Štěpnička P., Horáček M., Kubišta J., Varga V., Mach K.: *Collect. Czech. Chem. Commun.* **2008**, *73*, 967.

31. Nifantev I. E., Butakov K. A., Aliev Z. G., Urazovskii I. F.: *Metalloorg. Khim.* **1991**, *4*, 1265.
32. Nielson A. J., Schwerdtfeger P., Waters J. M.: *J. Chem. Soc., Dalton Trans.* **2000**, 529.
33. Kopf H., Pickardt J.: *Z. Naturforsch., B: Chem. Sci.* **1981**, *36*, 1208.
34. Bajgur C. S., Tikkanen W. R., Petersen J. L.: *Inorg. Chem.* **1985**, *24*, 2539.
35. Carpenter J. E., Weinhold F.: *Theochem, J. Mol. Struct.* **1988**, *169*, 41.
36. Dioumaev V. K., Rahimian K., Gauvin F., Harrod J. F.: *Organometallics* **1999**, *18*, 2249.
37. Dioumaev V. K., Harrod J. F.: *J. Organomet. Chem.* **1996**, *521*, 133.
38. Banovetz J. P., Stein K. M., Waymouth R. M.: *Organometallics* **1991**, *10*, 3430.
39. Li H., Gauvin F., Harrod J. F.: *Organometallics* **1993**, *12*, 575.
40. Grimmond B. J., Corey J. Y.: *Organometallics* **1999**, *18*, 2223.
41. Rosenberg L., Davis C. W., Yao J. Z.: *J. Am. Chem. Soc.* **2001**, *123*, 5120.
42. Curtis M. D., Epstein P. S.: *Adv. Organomet. Chem.* **1981**, *19*, 213.
43. Hao L. J., Woo H. G., Lebuis A. M., Samuel E., Harrod J. F.: *Chem. Commun.* **1998**, 2013.
44. Langmaier J., Samec Z., Varga V., Horáček M., Mach K.: *J. Organomet. Chem.* **1999**, *579*, 348.
45. Smith J. A., Brintzinger H. H.: *J. Organomet. Chem.* **1981**, *218*, 159.
46. Duff A. W., Kamarudin R. A., Lappert M. F., Norton R. J.: *J. Chem. Soc., Dalton Trans.* **1986**, 489.
47. Otwinowski Z., Minor W.: *Macromolecular Crystallography, Pt A*, Vol. 276, p. 307. Academic Press Inc., San Diego 1997.
48. Altomare A., Burla M., Camalli M., Cascarano G., Giacovazzo C., Guagliardi A., Moliterni A., Polidori G., Spagna R.: *J. Appl. Crystallogr.* **1999**, *32*, 115.
49. Sheldrick G. M.: *SHELXL97, Program for Crystal Structure Refinement from Diffraction Data*. University of Göttingen, Göttingen 1997.
50. Frisch M. J., Trucks G. W., Schlegel H. B., Scuseria G. E., Robb M. A., Cheeseman J. R., Montgomery J. A., Jr., Vreven T., Kudin K. N., Burant J. C., Millam J. M., Iyengar S. S., Tomasi J., Barone V., Mennucci B., Cossi M., Scalmani G., Rega N., Petersson G. A., Nakatsuji H., Hada M., Ehara M., Toyota K., Fukuda R., Hasegawa J., Ishida M., Nakajima T., Honda Y., Kitao O., Nakai H., Klene M., Li X., Knox J. E., Hratchian H. P., Cross J. B., Bakken V., Adamo C., Jaramillo J., Gomperts R., Stratmann R. E., Yazyev O., Austin A. J., Cammi R., Pomelli C., Ochterski J. W., Ayala P. Y., Morokuma K., Voth G. A., Salvador P., Dannenberg J. J., Zakrzewski V. G., Dapprich S., Daniels A. D., Strain M. C., Farkas O., Malick D. K., Rabuck A. D., Raghavachari K., Foresman J. B., Ortiz J. V., Cui Q., Baboul A. G., Clifford S., Cioslowski J., Stefanov B. B., Liu G., Liashenko A., Piskorz P., Komaromi I., Martin R. L., Fox D. J., Keith T., Al-Laham M. A., Peng C. Y., Nanayakkara A., Challacombe M., Gill P. M. W., Johnson B., Chen W., Wong M. W., Gonzalez C., Pople J. A.: *Gaussian 03*. Gaussian Inc., Wallingford (CT) 2004.